ACTA TECHNICA CORVINIENSIS
– Bulletin of Engineering
Tome X [2017]
Fascicule 4 [October – December]
ISSN: 2067 – 3809

[1.]O.A. OYEM, [2.]A.J. OMOWAYE, [2]O.K. KORIKO

THERMO-PHYSICAL EFFECTS OF THERMAL RADIATION AND HEAT GENERATION ON FREE CONVECTIVE HEAT AND MASS TRANSFER OVER A VERTICAL PLATE

[1.]Department of Mathematical Sciences, Federal University Lokoja, Kogi State, NIGERIA
[2.]Department of Mathematical Sciences, Federal University of Technology Akure, Ondo State, NIGERIA

Abstract: The thermo-physical effects of thermal radiation, heat generation and species concentration on Magneto-hydrodynamic free convective heat and mass transfer flow over a vertical plate with variable thermal conductivity is considered. The governing partial differential equations are transformed into coupled nonlinear ordinary differential equations with similarity transformations. The resulting coupled nonlinear differential equation is solved numerically by Runge-Kutta forth order with shooting technique. The effects of the thermo-physical properties on velocity, temperature and concentration profiles are illustrated graphically and numerical values of skin friction, Nusselt number and Sherwood number are presented in tables.
Keywords: MHD free convection; heat generation; thermal radiation; variable thermal conductivity; vertical plate

Introduction

The problem of fluid flow in an electromagnetic field has been studied for its importance in geophysics, metallurgy aerodynamic extrusion of plastic sheets and other engineering processes such as in petroleum engineering, chemical engineering, composite or ceramic engineering and heat exchanger (Sandeep and Sugunamma, 2013). Radiative convective flows are involved in countless industrial and environmental processes. For example, heating and cooling chambers, fossil fuel combustion energy process evaporation from large open water reservoirs, astrophysical flows, solar power technology and space vehicle re-entry. In the context of space technology and in processes involving high temperatures, the effects of radiation are of vital importance which has opened up to various investigators. Many researchers have investigated the interaction of thermal radiation, heat generation and free convection for different geometries, by considering various flow patterns. Muthucumaraswamy et al. (2006) investigated the effect of thermal radiation on the unsteady free convective flow over a moving vertical plate with mass transfer in the presence of a homogenous first order chemical reaction. Their result showed that velocity increases with decreasing radiation parameter or chemical reaction parameter. The interaction of free convection with thermal radiation of a viscous incompressible unsteady MHD flow past a moving vertical cylinder with heat and mass transfer was analysed by Reddy and Reddy (2009) and it was observed that when radiation parameter increases, the velocity and temperature decreases in the boundary layer. Khaleque and Samad (2010) studied radiation and viscous dissipation effects on a steady two-dimensional MHD free convection flow along a stretching sheet with heat generation. They observed that momentum boundary layer and the thermal boundary layer thickness reduce as a result of increasing radiation. Jana and Ghosh (2011) studied the effects of thermal radiation of a viscous incompressible fluid occupying a semi-infinite region of space bounded by an infinite horizontal moving hot flat plate in the presence of indirect natural convection by way of an induced pressure gradient. From their study, velocity slightly increases with increased radiation parameter as temperature increases with increasing values of

radiation parameter. Uddin and Kumar (2011) investigated the heat and mass transfer characteristics and the flow behaviour on MHD flow near the lower stagnation point of a porous isothermal horizontal circular cylinder. It was observed that with the increase in Schmidt number, skin friction and Nusselt number decreases while, Sherwood number increases.

Shit and Haldar (2012) studied the effect of thermal radiation and temperature dependent viscosity on free convective flow and mass transfer of an electrically conducting fluid over an isothermal sheet. The result of their study showed that effects of thermal radiation and variable viscosity can lead to the decrease of heat transfer, whereas, the presence of viscoelasticity of the fluid and magnetic field causes increase of heat transfer. Sandeep and Sugunamma (2013) analysed the effects of inclined magnetic field and radiation on free convective flow of dissipative fluid past a vertical plate through porous medium in the presence of heat source. Their results showed that decrease in inclination angle reduces the magnetic field effect but increase in radiation term does not show much effect on increase in skin friction, while, increase in heat source parameter causes the increase in velocity of fluid flow. Omowaye and Ajayi (2014) studied the effects of some thermo-physical properties on force convective stagnation point on a stretching sheet with convective boundary conditions in the presence of thermal radiation and magnetic field. They observed that increasing the value of magnetic field parameter resulted in the increase in skin friction coefficient, whereas, the Nusselt number decreases with increasing values of the magnetic parameter and radiation number.

A number of interesting applications of the principles of heat transfer are concerned with systems in which heat may be generated internally. Nuclear reactors, electrical conductors, exothermic and endothermic chemically reacting systems are some examples (Holman, 2002). Mixed convection MHD flow of nano-fluid over a non-linear stretching sheet with thermal radiation and suction and variable magnetic field is investigated by Keshtekar et al. (2014). Their results showed that thermal radiation, heat generation and the permeability parameter decreases with an increase in Prandtl number, suction and magnetic parameter. Animasaun and Oyem (2014) investigated the effect of variable viscosity, Dufour, Soret and thermal conductivity on free convective heat and mass transfer of non-Darcian flow past flat surface. Their result showed that with increase in Dufour and Soret Parameter, fluid velocity increases and temperature increases with increase in variation of Dufour but decreases with increase in Soret. Olajuwon and Baoku (2014) investigated the combined influence of internal heat generation, suction, thermal radiation and chemical reaction of nth order on an unsteady free convective heat and mass transfer flow of a chemically reactive third grade fluid over an infinite vertical porous plate with oscillating temperature applied to the plate. They noted that suction parameter has the influence of reducing velocity, temperature and species concentration fields, as the fluid velocity increases as the value of the second grade viscoelastic parameter increases.

GOVERNING EQUATION

A steady two-dimensional free convective heat and mass transfer fluid flow over a vertical plate with variable thermal conductivity, heat generation, thermal radiation and species concentration are considered. The flow in the x-axis is taken along the vertical plate in the upward direction and the y-axis is normal to the plate. Here, T_w and C_w are temperature and concentration of the fluid at the plate and T_∞ and C_∞ are the temperature and concentration outside the boundary layer as shown in figure 1.

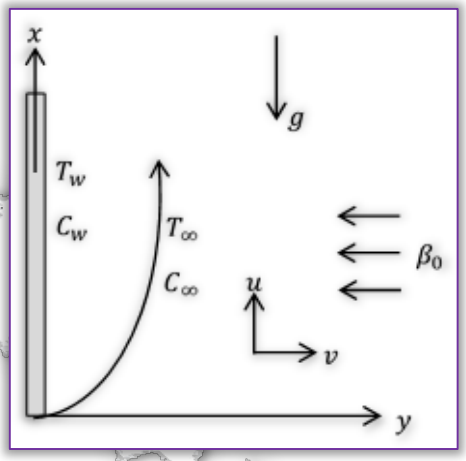

Figure 1. Problem schematics

Under the Boussinesq's approximation, the boundary layer is governed by the mass, momentum, energy and concentration equations as;

$$\frac{\partial u}{\partial x}+\frac{\partial v}{\partial y}=0 \quad (1)$$

$$u\frac{\partial u}{\partial x}+v\frac{\partial u}{\partial y}=\upsilon\frac{\partial^2 u}{\partial y^2}+g\beta(T-T_\infty)+g\beta^*(C-C_\infty)-\frac{\sigma\beta_0^2 u}{\rho} \quad (2)$$

$$u\frac{\partial T}{\partial x}+v\frac{\partial T}{\partial y}=\frac{1}{\rho c_p}\frac{\partial}{\partial y}\left(\kappa(T)\frac{\partial T}{\partial y}\right)-\frac{1}{\rho c_p}\frac{\partial q_r}{\partial y}+\frac{Q_0}{\rho c_p}(T-T_\infty) \quad (3)$$

$$u\frac{\partial C}{\partial x}+v\frac{\partial C}{\partial y}=D\frac{\partial^2 C}{\partial y^2} \quad (4)$$

The radiative heat flux q_r is describes by the Rosseland approximation given by

$$q_r=-\frac{4\sigma^*}{3k^*}\frac{\partial T^4}{\partial y} \quad (5)$$

where σ^* is the Stefan-Boltzmann constant and k^* is the Rosseland mean absorption coefficient. Following

Chamkha (1997), the temperature difference within the flow is assumed to be sufficiently small so that T^4 may be expressed as a linear function of temperature T. This is accomplished by expanding T^4 in a Taylor's series about the free stream temperature T_∞ such that

$$T^4 \approx 4T_\infty{}^3T - 3T_\infty{}^4 \quad (6)$$

In this research, the author shall assume that the fluid thermal conductivity κ vary as a linear function of temperature (Prasad et al. 2010) as

$$\kappa(T) = \kappa^*[1 + \delta^*(T - T_\infty)] \quad (7)$$

where κ(T) is the thermal conductivity of the fluid depending on the fluid temperature T and δ^* being a constant which may either be positive or negative. In this research, $\delta > 0$ is thermal conductivity generation and κ^* is the thermal conductivity of the ambient fluid.

The corresponding boundary conditions are

$$u = 0 \;\; v = 0 \;\; T = T_w \;\; C = C_w \;\; \text{at } y = 0$$
$$u \to 0 \;\; T \to T_\infty \;\; C \to C_\infty \;\; \text{as } y \to \infty \quad (8)$$

The velocity components along the axes can be expressed as:

$$u = \frac{\partial \psi}{\partial y} \quad \text{and} \quad v = -\frac{\partial \psi}{\partial x} \quad (9)$$

substituting equation (9) into equation (1), equation (1) is satisfied. Defining similarity variable and the dimensionless variables as

$$\eta = y\sqrt{\frac{U_0}{2\upsilon x}}, \theta(\eta) = \frac{T - T_\infty}{T_w - T_\infty},$$
$$\phi(\eta) = \frac{C - C_\infty}{C_w - C_\infty}, \psi = \sqrt{2x\upsilon U_0}\, f(\eta) \quad (10)$$

where ψ is the stream function, f is dimensionless velocity, θ is the dimensionless fluid temperature and ϕ is the dimensionless concentration. Introducing equation (10) into equations (1)-(9), the coupled nonlinear ordinary differential equation is obtained

$$f''' + ff'' + Gr\theta + Gm\phi - Mf' = 0 \quad (11)$$
$$\left(1 + \gamma\theta + \frac{4}{3N}\right)\theta'' + Prf\,\theta' + \gamma\theta'^2 + PrQ\theta = 0 \quad (12)$$
$$\phi'' + Scf\phi' = 0 \quad (13)$$

subject to the boundary conditions

$$\eta = 0 ; \;\; f = 0 \;\; f' = 0 \;\; \theta = 1 \;\; \phi = 1$$
$$\eta \to \infty ; \;\; f' \to 0 \;\; \theta \to 0 \;\; \phi \to 0 \quad (14)$$

Equations (11) – (13) with boundary conditions (14) describe the heat and mass transfer over a vertical plate in the presence of magnetic field under variable thermal conductivity, thermal radiation, heat generation and species concentration. It is noteworthy that the local parameters Gr, Gm, M and Q in equations (11) – (13) are functions of x. Here, prime denotes the differentiation with respect to η and:

$Gr = \frac{2xg\beta(T_w - T_\infty)}{U_0^2}$ (local thermal Grashof number),

$Gm = \frac{2xg\beta^*(C_w - C_\infty)}{U_0^2}$ (local modified thermal Grashof number),

$M = \frac{2x\sigma\beta_0^2}{\rho U_0}$ (local magnetic field parameter),

$Pr = \frac{\upsilon}{\alpha}$ (Prandtl number),

$Q = \frac{2xQ_0}{\rho c_p U_0}$ (heat generation parameter),

$Sc = \frac{\upsilon}{D}$ (Schmidt number),

$\gamma = \delta(T_w - T_\infty)$ (variable thermal conductivity parameter),

$N = \frac{\kappa\kappa^*}{4\sigma^* T_\infty^3}$ (thermal radiation parameter of the flow).

NUMERICAL COMPUTATION

The set of equations (11) - (13) under the boundary conditions (14) are solved numerically by Runge-Kutta forth order technique with shooting method. The basic idea is to reduce the higher order nonlinear differential equations (11) - (13) to system of first order linear differential equations and they are further transformed into initial value problem and then apply shooting technique with Gr, Gm, M, Pr, Q, Sc, γ and N as prescribed parameters. The results are presented in figures 2 - 25.

Let $f = x_1, f' = x_2, f'' = x_3, \theta = x_4, \theta' = x_5, \phi = x_6, \phi' = x_7$. Then equations (11) – (14) are transformed into a system of first order differential equations as:

$$x_1' = x_2$$
$$x_2' = x_3$$
$$x_3' = Mx_2 - Grx_4 - Gmx_6 - x_1x_3$$
$$x_4' = x_5$$
$$x_5' = \left(\frac{3N}{3N(1 + \gamma x_4) + 4}\right)(-Prx_1x_5 - \gamma x_5^2 - PrQx_4) \quad (15)$$
$$x_6' = x_7$$
$$x_7' = -Scx_1x_7$$

subject to the following initial conditions:

$$x_1(0) = 0, x_2(0) = 0, x_3(0) = s_1, x_4(0) = 1,$$
$$x_5(0) = s_2, x_6(0) = 1, x_7(0) = s_3 \quad (16)$$

The computations are carried out by a program which uses a symbolic and computational computer language MATLAB with a step-size of $\Delta\eta = 0.001$, chosen to satisfy the convergence criterion of 10^{-6}. From the process of computation, the skin friction coefficient $f''(0)$, Nusselt number $-\theta'(0)$ and mass transfer coefficient in terms of Sherwood number $-\phi'(0)$ respectively are also worked out and their numerical values are presented in a tables 1 – 3.

RESULTS AND DISCUSSION

In order to get a physical insight into the problem, velocity, temperature and concentration profiles have been computed and displayed graphically. Skin-friction coefficient, Nusselt and Sherwood numbers are also computed for various values of the governing parameters: thermal radiation parameter(N), local thermal Grashof number (Gr), local modified thermal Grashof number (Gm), Prandtl number (Pr), local

magnetic field parameter (M), Schmidt number (Sc), heat generation parameter (Q) and variable thermal conductivity parameter (γ).

The velocity, temperature and concentration profiles are displayed in figures 2 – 4 respectively. It was observed from figure 2 that as γ increases in value, velocity increases steeply to a peak along the plate and decreases gradually away from the plate towards the free stream. In figure 4, concentration profiles decreases with an increase in variable thermal conductivity, while, in figure 3, temperature profiles increases with increasing values of thermal conductivity variation parameter γ.

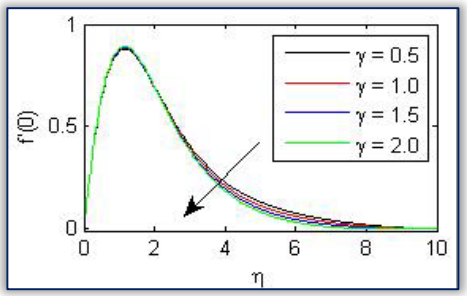

Figure 2: Velocity profiles over a vertical plate for various values of variable thermal conductivity γ

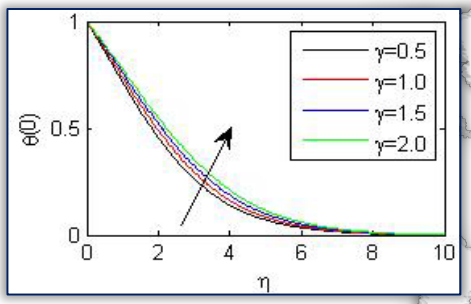

Figure 3: Temperature profiles over a vertical plate for various values of thermal conductivity variation parameter γ

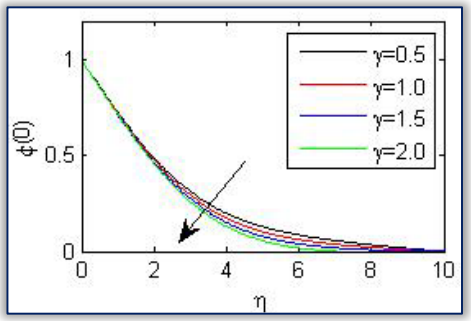

Figure 4: Concentration profiles for various values of γ

Prandtl number Pr is found to be the parameter that relates the relative thickness of the hydrodynamic and thermal boundary layer. Thereby making it the link between the velocity and the temperature fields (Holman, 2004). The effects of Prandtl number Pr on velocity, temperature and concentration distributions are displayed in figures 5, 6 and 7 respectively. Figures 5 and 6 shows that velocity and concentration profiles increases with the increase in Prandtl number Pr. It was also observed in figure 5 that there was an initial rise at $Pr = 0.71, 1.0$ and later, a sharp rise in velocity and concentration boundary layers away from the plate towards the free stream was observed at$Pr = 3.0$. Figure 6 shows that temperature profiles decreases as Prandtl number Pr increases. It is also interesting to note that increase in Pr means a decrease in variable thermal conductivity.

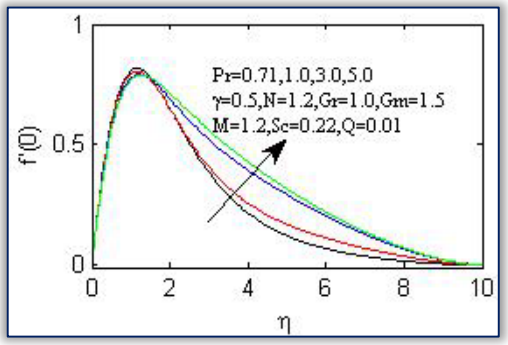

Figure 5: Prandtl number (Pr) effects on velocity profiles

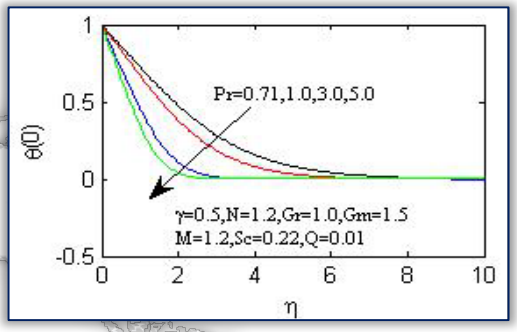

Figure 6: Prandtl number (Pr) effects on temperature profiles

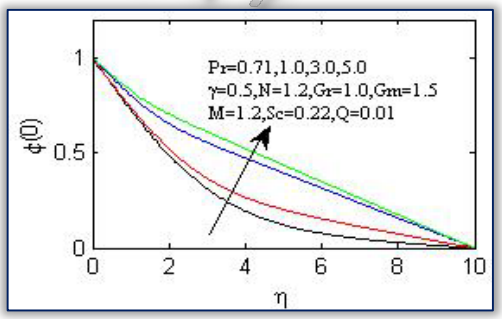

Figure 7: Prandtl number (Pr) effect on concentration profiles

It was observed from figure 6 that for $Pr = 0.71, 1.0$, there is a slight rise in the thermal boundary layers near the plate but decreases sharply for $Pr = 3.0$ towards the plate (Khaleque and Samad, 2010). In figure 7, increase in Prandtl number results in the increase in concentration profiles. It was observed that it increases sharply away from the plate towards the free stream.

Figures 8 - 10 shows the variation of velocity, temperature and concentration profiles respectively with local thermal Grashof number (Gr). From figure 8,

it was observed that velocity profiles increases spontaneously at an initial state near the vertical plate as local thermal Grashof number increased but moving away from the plate, a cross flow in the velocity is induced as velocity gently decreases away from the plate at a slower rate with increasing values of Gr. Since Gr > 0 corresponds to externally cooled plate, substantial increase in velocity distribution profiles is observed near the plate, thereby indicating greater cooling results in velocity increase and thermal boundary layer thickness. This situation reveals that the buoyancy force accelerates the velocity field and no flow reversal occurs to prevent separation (Khaleque and Samad, 2010, Jana and Ghosh, 2011).

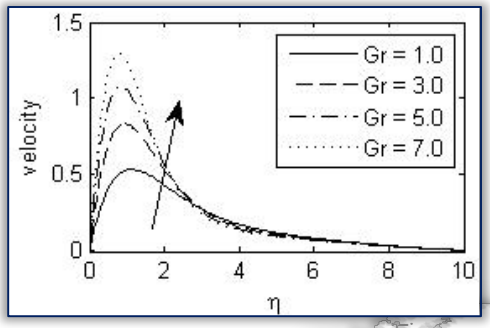

Figure 8: Grashof number (Gr) effect on velocity profiles

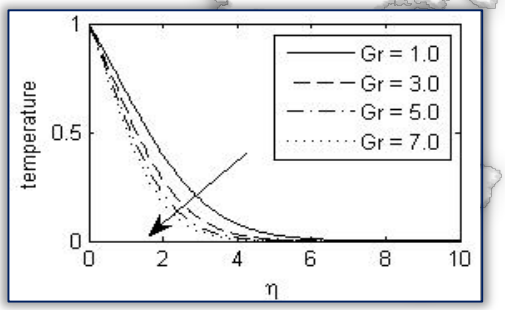

Figure 9: Grashof number (Gr) effect on temperature profiles

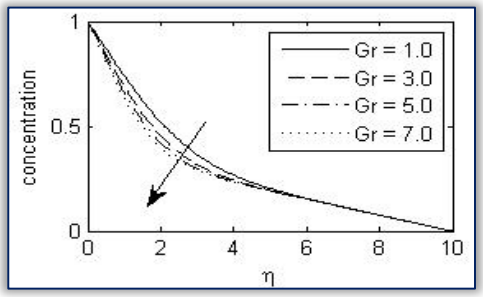

Figure 10: Grashof number (Gr) effect on concentration profiles

From figures 9 and 10, the thermal boundary layer on temperature profiles and concentration boundary layers reduces with increasing values of Gr, causing the fluid temperature to reduce at every point other than the plate. When a heated surface is in contact with the fluid, the result of temperature difference causes buoyancy force, which induces the natural convection (Abah et al. 2012).

Velocity, temperature and concentration distribution profiles for different values of thermal radiation parameter with Gr = 1.0, γ = 0.5, Sc = 0.2, Q = 0.01, Gm = 1.5, Pr = 0.71, M = 1.2 are displayed in figures 11, 12 and 13. It was observed from figure 11 that velocity profiles increases initially to a peak near the plate as η increases but decreases away towards the free stream as the thermal radiation parameter N increases. It also reveals that increasing values of N causes less interaction of radiation with the momentum boundary layer.

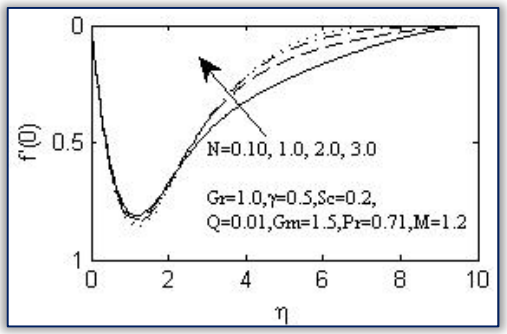

Figure 11: Velocity profiles against η for varying values of N

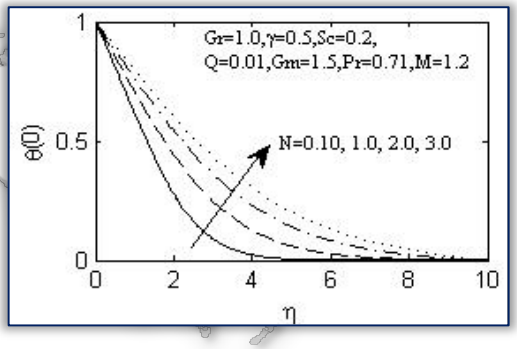

Figure 12: Temperature profiles against η for various values of thermal radiation parameter N

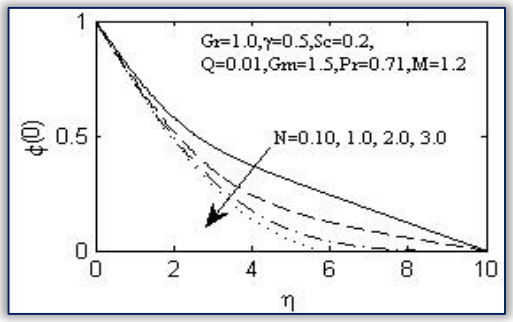

Figure 13: Concentration profiles for various values of thermal radiation parameter N

Figure 12 reveals that temperature profiles increase as radiation parameter N increases. This is because thermal radiation in the fluid increases the temperature within the boundary layer which accelerates the convection as well as increases the flow within the boundary layer. It was observed from figure 13 that the concentration profiles decreases in boundary layers away from the plate as thermal radiation parameter

increases. However, this result shows that concentration boundary layer thickness can be reduced as a result of increase in thermal radiation parameter N.

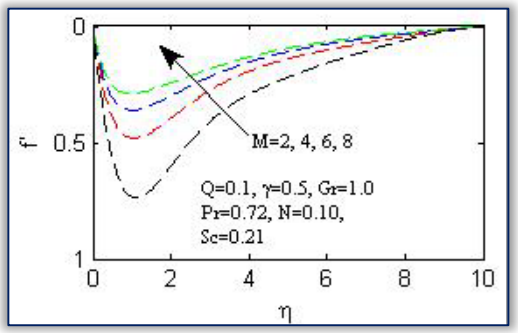

Figure 14: Variation of f′(η) with η for different values of M

For different values of the local magnetic parameter M, velocity profiles are plotted in figure 14. It was observed that velocity attains maximum point near the plate at low local magnetic parameter and decreases freely as M increases across the boundary layer because of the application of transfer magnetic field which tends to resist the fluid flow. Consequently, the boundary layer thickness decreases with an increase in the local magnetic field while, the separation of the boundary layer occurs earlier and the momentum boundary layer becomes thicker. But the reverse is observed within the boundary layer for temperature and concentration profiles as shown in figures 15 and 16.

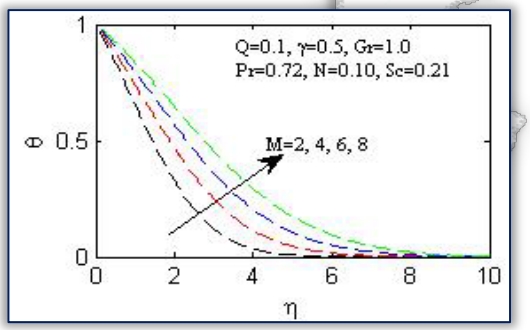

Figure 15: Temperature profile θ(η) with η for different values of M

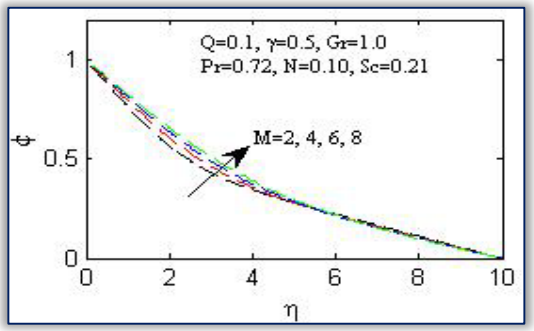

Figure 16: Variation of ϕ(η) with η for different values of M

It was observed that increasing local magnetic field, the temperature of the fluid increases while and concentration species has an enhanced effect on the flow from the plate to the free stream (Shit and Haldar, 2012).

Figure 17 presents the velocity profiles for various values of local modified thermal Grashof number (Gm). It was observed that increase in the values of Gm, have the tendency to induce more flow in the boundary layer due to the effect of thermal buoyancy, thereby producing an increase in velocity flow (Abah et al. 2012).

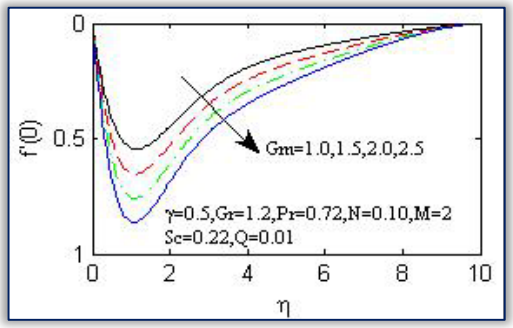

Figure 17: Velocity profiles f′(η) against η for different values of modified thermal Grashof number

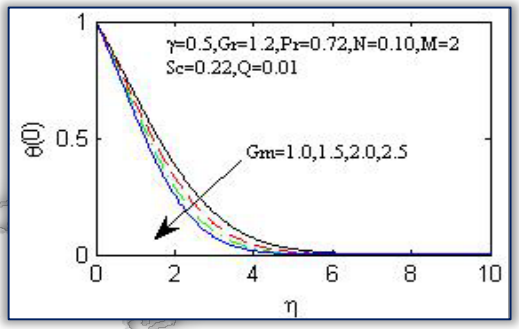

Figure 18: Temperature profiles θ(η) against η for various Values of modified thermal Grashof number Gm

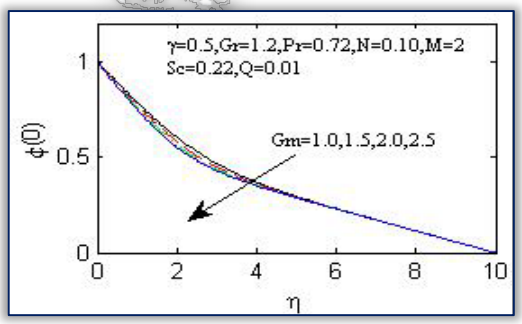

Figure 19: Concentration profiles θ(η) against η for various Values of modified thermal Grashof number Gm

Temperature and concentration profiles for Gm are presented in figures 18 and 19. It was observed that increasing the values of modified thermal Grashof number, both temperature and concentration profiles decreases gradually towards the free stream. Figures 20 – 22 shows the effects of Schmidt number Sc on velocity, temperature and concentration profiles. From figures 20 and 22, we observed that velocity and concentration profiles decreases respectively as Schmidt number Sc increases. We also observed from figure 20 that after an initial rise from zero to a peak in the velocity profile, Sc decreases greatly away from the plate. Meanwhile, temperature profiles increases gradually away from the

plate as the Schmidt number Sc increases in values as shown in figure 21.

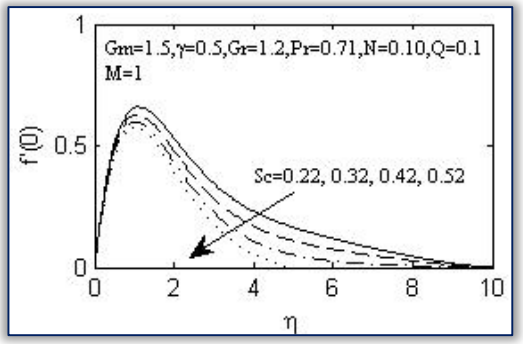

Figure 20: Velocity profiles for various values of Schmidt number Sc

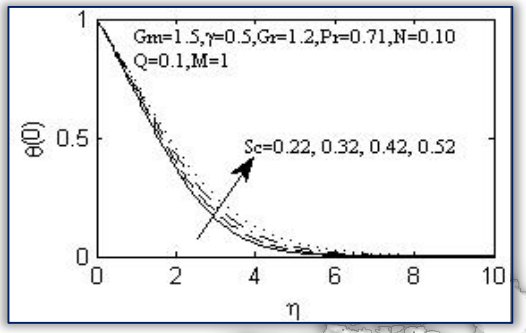

Figure 21: Temperature profiles for various values of Schmidt number Sc

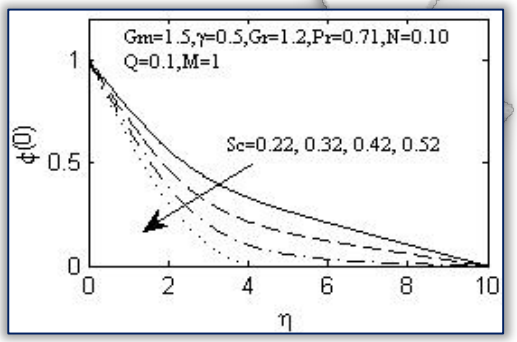

Figure 22: Concentration profiles for various values of Schmidt number Sc

The effects of heat source parameter Q on velocity, temperature and concentration boundary layers are displayed respectively in figures 23 – 25. From figures 23 and 24, it was observed that velocity and temperature profiles increases as heat source parameter Q increases. While, from figure 25, concentration profiles decreases with increase in heat generation parameter Q. Also, it was observed from figures 23 – 25, that for various values of $Q = 0.01, 0.04, 0.08, 0.1$, there was little but significant variations in the corresponding velocity, temperature and concentration profiles. However, the concentration boundary layer thickness reduces as a result of the increase in the heat source parameter Q and also shows that large values of heat source parameter Q have significant effect on velocity and temperature distributions.

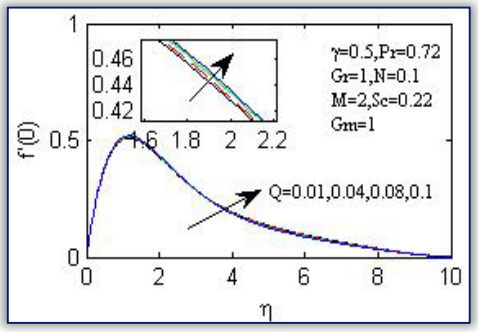

Figure 23: Velocity profiles for various values of Q

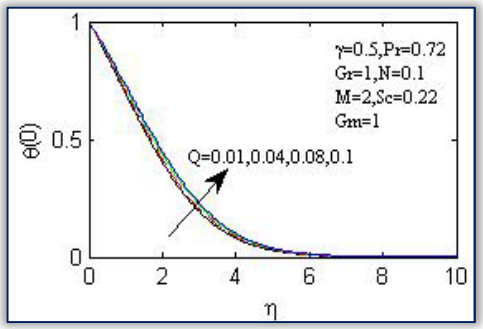

Figure 24: Temperature profiles for various values of Q

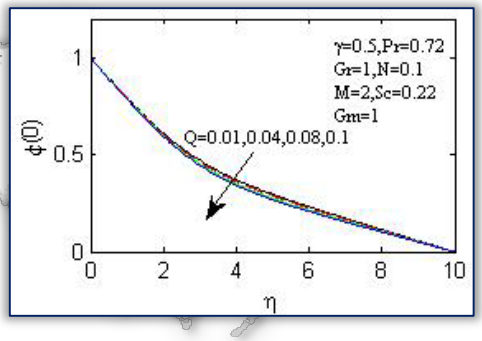

Figure 25: Concentration profiles for various values of Q

Numerical values of skin friction coefficient, rate of heat transfer and mass transfer are presented in tables 1 – 3. The effects of Pr, γ, N, Gr, Gm, M, Sc, and Q on the Skin friction (C_f) are numerically shown in Table 1. We observed that shear stress in terms of skin friction coefficient increases slightly as variable thermal conductivity (γ) increases but decreases with increase in Schmidt number, Prandtl number and local magnetic field parameter. It is observed that as buoyancy parameter and thermal radiation parameter increases, the skin friction coefficient increases. Similarly, we observed that a decrease in the modified thermal Grashof number Gm heat source parameter Q leads to a decrease in skin friction. The effects of Pr, γ, N, Gr, Gm, M, Sc, and Q on the rate of heat transfer in terms of Nusselt number are shown in Table 2. It is seen that as γ, N, Gr, Gm, and Q increases, the rate of heat transfer decreases. Also, as Prandtl number increase, the Nusselt number increases, whereas, it decreases with decreasing values in local magnetic field and Schmidt number respectively.

Table 1: Numerical values of shear stress in terms of skin friction (C_f)

γ	Pr	Gr	N	M	Gm	Sc	Q	C_f
0.5	0.71	1.0	1.2	1.0	1.5	0.22	0.01	1.8197
1.0								1.8258
1.5								1.8316
2.0								1.8371
0.5	0.71	1.0	1.2	1.2	1.5	0.22	0.01	1.7351
	1.0							1.7198
	3.0							1.6836
	5.0							1.6618
0.5	0.72	1	0.10	2	1.2	0.32	0.01	1.2612
		3						2.2405
		5						3.1447
		7						3.9984
0.5	0.71	1.0	0.1	1.2	1.5	0.2	0.01	1.7227
			1.0					1.7437
			2.0					1.7647
			3.0					1.7804
0.5	0.72	1.0	0.10	2	2.0	0.21	0.1	1.7418
				4				1.3417
				6				1.1332
				8				0.9998
0.5	0.72	1.2	0.10	2	1.0	0.22	0.01	1.2757
					1.5			1.5542
					2.0			1.8311
					2.5			2.1065
0.5	0.71	1.2	0.10	1	1.5	0.22	0.1	1.5649
						0.32		1.5323
						0.42		1.5045
						0.52		1.4816
0.5	0.72	1	0.10	2	1.0	0.22	0.01	1.1715
							0.04	1.1754
							0.08	1.1809
							0.10	1.1838

Table 2: The rate of heat transfer in terms of Nusselt number (Nu)

γ	Pr	Gr	N	M	Gm	Sc	Q	Nu
0.5	0.71	1.0	1.2	1.0	1.5	0.22	0.01	0.2781
1.0								0.2510
1.5								0.2296
2.0								0.2122
0.5	0.71	1.0	1.2	1.2	1.5	0.22	0.01	0.2695
	1.0							0.3241
	3.0							0.5427
	5.0							0.6686
0.5	0.72	1	0.10	2	1.2	0.32	0.01	0.3002
		3						0.3747
		5						0.4256
		7						0.4652
0.5	0.71	1.0	0.1	1.2	1.5	0.2	0.01	0.3699
			1.0					0.2861
			2.0					0.2345
			3.0					0.2040
0.5	0.72	1.0	0.10	2	2.0	0.21	0.1	0.3142
				4				0.2331
				6				0.1795
				8				0.1393
0.5	0.72	1.2	0.10	2	1.0	0.22	0.01	0.3056
					1.5			0.3365
					2.0			0.3637
					2.5			0.3881
0.5	0.71	1.2	0.10	1	1.5	0.22	0.1	0.2882
						0.32		0.2738
						0.42		0.2586
						0.52		0.2424
0.5	0.72	1	0.10	2	1.0	0.22	0.01	0.2958
							0.04	0.2789
							0.08	0.2551
							0.10	0.2427

Table 3: Numerical values of mass transfer in terms of Sherwood number (Sh)

γ	Pr	Gr	N	M	Gm	Sc	Q	Sh
0.5	0.71	1.0	1.2	1.0	1.5	0.22	0.01	0.2828
1.0								0.2881
1.5								0.2923
2.0								0.2956
0.5	0.71	1.0	1.2	1.2	1.5	0.22	0.01	0.2747
	1.0							0.2618
	3.0							0.2046
	5.0							0.1804
0.5	0.72	1	0.10	2	1.2	0.32	0.01	0.2616
		3						0.3148
		5						0.3513
		7						0.3798
0.5	0.71	1.0	0.1	1.2	1.5	0.2	0.01	0.2338
			1.0					0.2591
			2.0					0.2691
			3.0					0.2729
0.5	0.72	1.0	0.10	2	2.0	0.21	0.1	0.2394
				4				0.2083
				6				0.1893
				8				0.1762
0.5	0.72	1.2	0.10	2	1.0	0.22	0.01	0.2137
					1.5			0.2289
					2.0			0.2422
					2.5			0.2542
0.5	0.71	1.2	0.10	1	1.5	0.22	0.1	0.2368
						0.32		0.2907
						0.42		0.3392
						0.52		0.3821
0.5	0.72	1	0.10	2	1.0	0.22	0.01	0.2089
							0.04	0.2115
							0.08	0.2151
							0.10	0.2170

Similarly, numerical values on the effects of the prescribed parameters on Sherwood number Sh are shown in table 3. It was observed that rate of mass transfer coefficient increases with increasing values of γ, M and Pr but decreases as Gr, Gm, N, Sc and Q increases in values.

SUMMARY AND CONCLUSION

The problem on thermo-physical effects of thermal radiation and heat generation on free convective heat and mass transfer over a vertical plate is considered. The governing partial differential equations of the problem, using similarity transformations, were reduced to coupled nonlinear ordinary differential equations and solved numerically using Runge-Kutta fourth order method with shooting technique. The effects of local magnetic parameter, Prandtl number, local thermal Grashof number, modified local thermal Grashof number, heat generation parameter, variable thermal conductivity, Schmidt number and radiation parameter on velocity, temperature and concentration profiles are presented. From the results, the following conclusions are drawn:

i). The skin friction and Nusselt number increase with increasing values of γ, N, and Q, but decreases in Sherwood number. An increase in Pr, M and Sc cause an increase in Nusselt number and Sherwood number and decreases in the skin

friction. Similarly, Sherwood and Nusselt number decreases with increasing values of Gm and Gr but increases in the skin friction.

ii). The velocity boundary layer thickness decreases with γ, N, M, Sc

iii). The thermal boundary layer thickness increases with γ, N, M, Sc, Q and decreases with Pr, Gr, Gm

iv). The species concentration decreases with γ, Gr, N, Gm, Sc, Q but decreases with increasing values in Pr, M.

Acknowledgement

I would like to acknowledge Prof. Koriko O. K. and Dr. A. J. Omowaye of the Department of Mathematical Sciences of Federal University of Technology Akure for their constructive assessment towards the successful completion of the research.

References

[1.] Abah, S.O., Eletta, B.E., Omale, S.O.: The numerical analysis of the effect of free convection heat and mass transfer on the unsteady boundary layer flow past a vertical plate. International J. of Theo. and Math. Phys., 2(3), pp. 33-36, (2012)

[2.] Animasaun, I.L., Oyem, O.A.: Effect of variable viscosity, dufour, soret and thermal conductivity on free convective heat and mass transfer of non-darcian flow past porous flat surface. American J. of Comp. Math., 4, pp. 357-365, (2014), doi.org/10.4236/ajcm.2014.44030

[3.] Chamkha, A.J.: Hydromagnetic natural convection from an isothermal inclined surface adjacent to a thermally stratified porous medium. Int. J. Eng. Sci., 35(10), pp.975-986, (1997)

[4.] Holman, J.P.: Heat Transfer (ninth edition), Tata McGraw-Hill Publishing Company Limited, New Delhi, (2004)

[5.] Jana, R.N., Ghosh, S.K.: Radiative heat transfer of an optically thick gray gas in the presence of indirect natural convection. World J. of Mechanics, 1, pp. 64-69, (2011)

[6.] Keshtekar, M.M., Khaluei, A., Fard, H.A.: Effects of thermal radiation, viscous dissipation, variable magnetic field and suction on mixed convection MHD flow of nanofluid over a non-linear stretching sheet. IOSR J. of Eng., 4(5), pp. 44-54, (2014)

[7.] Khaleque, T.S., Samad, M.A.: Effects of radiation, heat generation and viscous dissipation on MHD free convection flow along a stretching sheet. Research J. of Appl. Sci., Eng. and Tech., 2(4), pp. 368-377, (2010)

[8.] Mathucumaraswamy, R, Chandrakala, P., Anthony Raj, S.: Radiative heat and mass transfer effects on moving isothermal vertical plate in the presence of chemical reaction. Int. J. of Appl. Mech. and Eng., 11(3), pp. 639-646, (2006)

[9.] Omowaye, A.J., Ajayi, A.O.: Effects of some thermo-physical properties on force convective stagnation point on a stretching sheet with convective boundary conditions in the presence of thermal radiation and magnetic field. Math Theory and Modeling, 4(9), pp. 24-30, (2014)

[10.] Prasad, K.V., Vajravelu, K., Datti, P.S.: The effects of variable fluid properties on the hydromagnetic flow and heat transfer over a non-linearly stretching sheet. Int. J. of Thermal Sci., 49, pp. 603–610, (2010)

[11.] Reddy, M.G., Reddy, N.B.: Radiation and mass transfer effects on unsteady MHD free convection flow of an incompressible viscous fluid past a moving vertical cylinder. Theoret. Appl. Mech. Belgrade, 36(3), pp. 239-260, (2009)

[12.] Sandeep, N., Sugunamma, V.: Effect of inclined magnetic field on unsteady free convective flow of dissipative fluid past a vertical plate. Open J. of Adv. Eng. Tech., 1(1), pp. 6-23, (2013)

[13.] Shit, G.C., Haldar, R.: Thermal radiation effects on MHD viscoelastic fluid flow over a stretching sheet with variable viscosity. Int. J. of Appl. Math and Mech., 8(14), pp. 14-36, (2012)

[14.] Uddin, Z., Kumar, M.: MHD heat and mass transfer free convection flow near the lower stagnation point of an isothermal cylinder imbedded in porous domain with the presence of radiation. Jordan J. of Mech. and Ind. Eng., 5(2), pp. 133-138, (2011)

ISSN:2067-3809